Cornell University

Biological and Environmental Engineering
"We Bring Engineering to Life"

Cold Therapy of Sporting Injury in Upper Thigh Region

A Comprehensive Study on the Time Required to achieve Optimal Cooling and the Effects of Swelling

By:
Jack Chen
Ian Chiang
Alex Hu
David Huland
Paul Youn

Executive Summary

One of the most common injuries amongst athletes is soft tissue injury due to impact, and the traditional treatment for this is cold therapy using an ice pack. While this treatment is effective, inexpensive, and easily accessible, there is very little quantitative data available on the actual effects of ice on the muscle. The most common advice found in medical textbooks and literature is a 20 minute on, 20 minute off icing cycle. In this study we model the temperature distribution in the upper leg region after one and a half cycles of ice therapy. Our axisymmetric model consists of three layers: skin, fat, and muscle, and we include an initial swelling of the muscle layer that decreases as a function of the muscle temperature. After an initial 20 minutes of cooling, the desired temperature change of 10°C penetrated to only 4 mm into the muscle layer, but after a 60 minute cycle, the desired cooling increased to 1 cm. Our sensitivity analysis revealed that slight changes in properties such as density, specific heat and conductivity did not alter the results significantly. Also, using a fixed muscle thickness independent of temperature yielded a lower temperature drop in the muscle layer. It was concluded that ice therapy, though slow, is effective in cooling some of the muscle to the desired temperature, and its main advantages stem from its inexpensiveness and ease of application.

Key Words: sports injury, soft tissue injury, muscle injury, cold therapy, COMSOL, heat transfer.

Introduction and Design Objectives:

Introduction

One of the most common injuries amongst athletes is soft tissue injury due to impact. Typically, as a result of impact, cells in the underlying muscle tissue rupture, causing a bruise, while the cells of the skin and fat layers remain undamaged. For treatment of these common soft tissue injuries, cold therapy has been used for thousands of years, and while any physician today will agree that it is effective, there is very little data and even fewer studies on the actual effects of putting ice on an injured site. Because of this, recommendations for the duration of application vary from physician to physician and even in medical textbooks. In this project, we hope to examine the effect of applying ice on soft tissue injury in the leg by modeling this process in COMSOL. To create a realistic model, we will consider factors such as metabolic heat generation and swelling due to impact.

Design Objective

In our study, we create a comprehensive heat transfer model that allows us to assess the effectiveness of a 20 minute icing treatment of injured muscle tissue. In previous research, it was suggested that treatment should result in lowering the muscle temperature by 10-15^{o}C. However, few clinicians can give specific evidence as to the appropriate duration of each individual treatment session. In this study, we model the

temperature profile of a 20 minute icing cycle; we wish to determine how deep the cooling front penetrates into the injured muscle during this time period. In the case of physical trauma, tissues undergo swelling, which subsides during the icing cycle. Hence, we model the heat transfer profile with a varying thickness of the muscle layer during the cooling cycle. In designing the anatomical layout of the injured site, we use COMSOL to set up an axi-symmetric model of a human leg. Following meshing the geometry, we model the heat transfer process under different conditions.

Assumptions

To develop a manageable model that closely resembles the complex process of cooling human tissue, various assumptions are made. First, the lateral heat transfer out of the tissue is assumed to be negligible. Ice is modeled as a boundary condition, assumed to remain at 273 K, since the energy required to melt the entire ice and raise the temperature of the liquid is extremely high. Finally, the heat flux at muscle-bone boundary is assumed to be zero, considering the bone as an insulator. Thermal properties of all layers are assumed to be constant. Volumetric blood rate, and hence heat generation, in muscle tissue is constant, while that in skin and fat layer is zero. No plausible quantitative model for muscle swelling exists. Therefore, we use empirical data to model the contraction of the muscle, assuming a linear relationship between temperature and muscle thickness.

Schematic

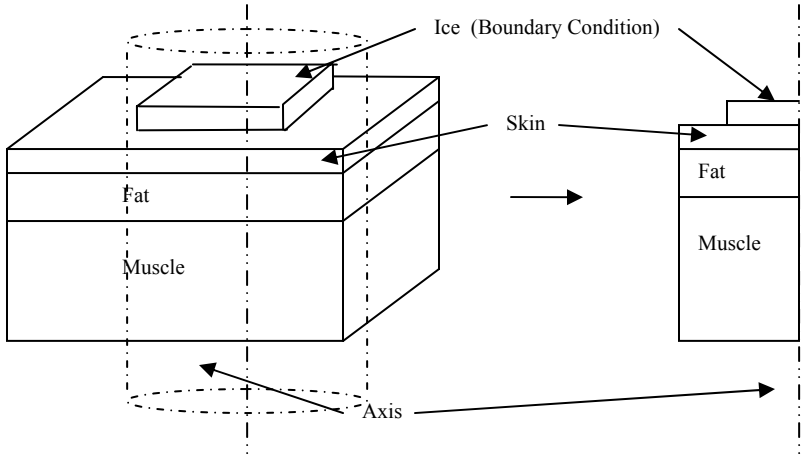

Dimensions (not labeled on diagram):

Length of radius: 5 cm
Thickness of skin (sum of epidermis, dermis, subcutaneous tissue): 3 mm
Thickness of fat: 5 mm
Thickness of muscle (hamstring): 6 cm

At t = 0, the muscle is in swelled state. The thickness of the muscle is a function of the temperature given as follows:

$$dL=L_0*\alpha*dT$$

Results and Discussion:

Analytical Solutions

Geometry & Mesh

Using COMSOL Multiphysics, we created a dynamic mesh based on our schematics (**Figure 1**). The boundary conditions and initial conditions were programmed as mentioned above. Our geometry simplified the 3-D physical problem to a 2-D axisymmetric model, in which we focus on the swelling site of the upper thigh region. The bottom 2 cm of the model is omitted in our results for aesthetic purposes. The temperature of the bottom layer did not change at any given time throughout the 20 minutes cooling period. The non-uniformity of the mesh was created by the COMSOL program to optimize the calculation. The mesh was created so as to be precise enough for our model without excessive calculation time (**Figure 2**).

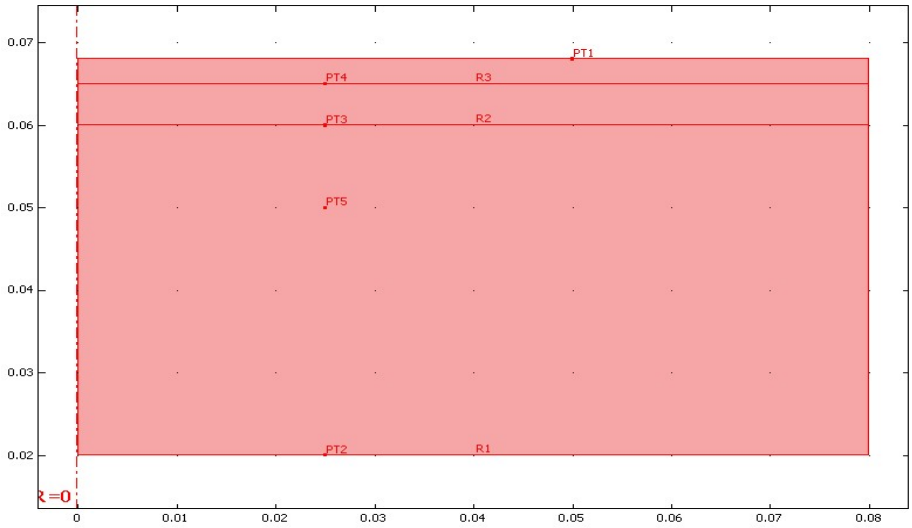

Figure 1: Geometry of the schematic model. The X and Y axis scales are in meters. PT1 marks the end of ice pack. The top layer models the skin, the middle layer models the fat and the bottom layer models the muscle.

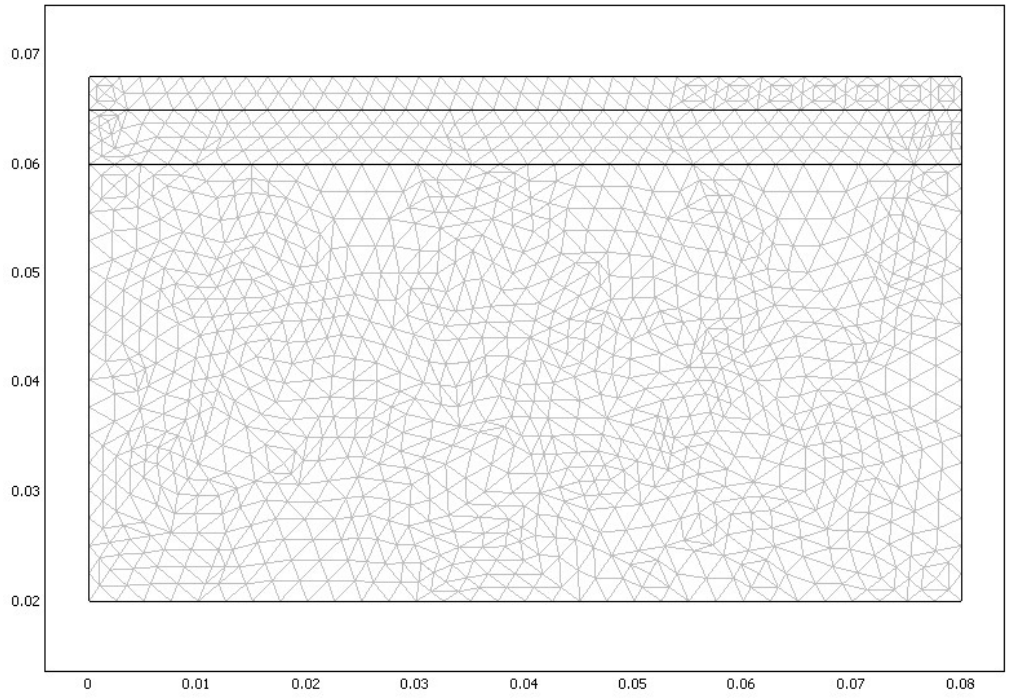

Figure 2: Mesh of the schematic region. The X and Y axes are in meters. The top layer models the skin, the middle layer models the fat and the largest bottom layer models the muscle.

Modeling

To model the effectiveness of cold therapy for an upper thigh injury due to a sporting injury, we used our mesh and modeled the temperature profile at different time points. The muscle part of our mesh changed its thickness based on the change of temperature (See Appendix). The temperature profile of our model at the starting point (t = 0) was uniform within each layer (**Figures 3 & 4**). This simplified the initial conditions, while still accounting for slight temperature variations within the various layers.

As the cooling process continued, the temperature at different layers changed and the swelling subsided. At the end of the 20 minutes cooling process, the muscle layer contracted by one centimeter.

At the end of 20 minutes of cooling, the desired drop in temperature of 10^{o}C penetrated only 4 mm into the muscle layer (**Figures 5 & 6**). The temperature changes throughout the cooling process at different boundaries are shown in **Figure 7**. Therefore, it can be seen that the 10^{o}C cooling was only achieved in the very near proximity of the fat-muscle boundary after a single 20 minute application of the ice pack.

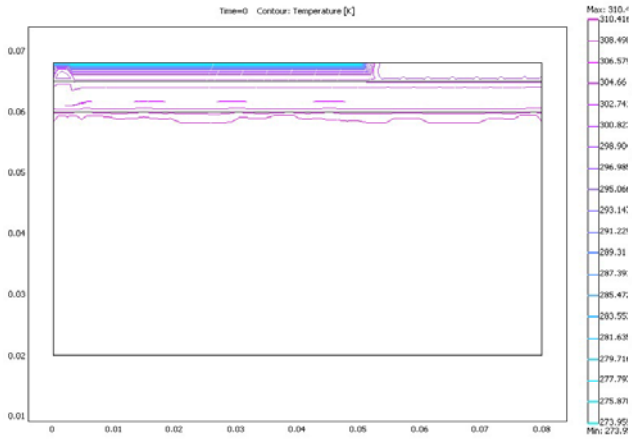

Figure 3: Temperature contour at time = 0.

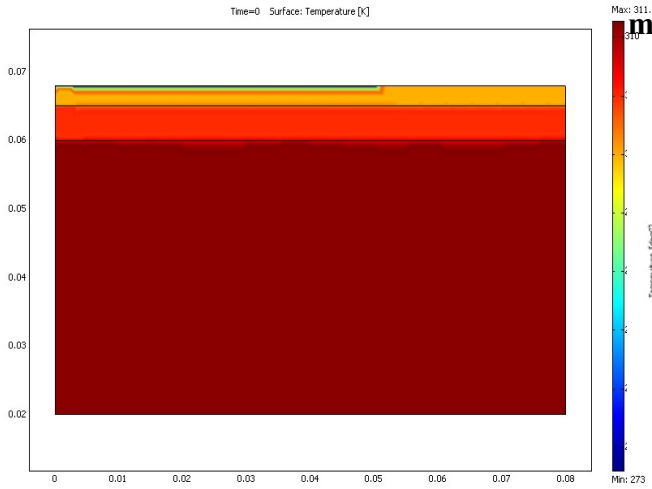

Figure 4: Temperature profile at t = 0.

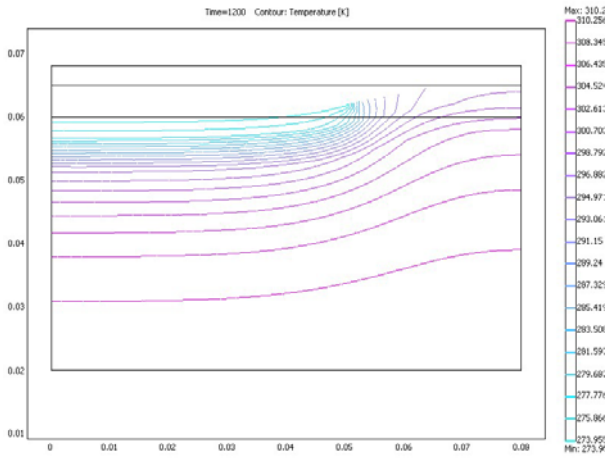

Figure 5: Temperature contour at time = 1200 seconds

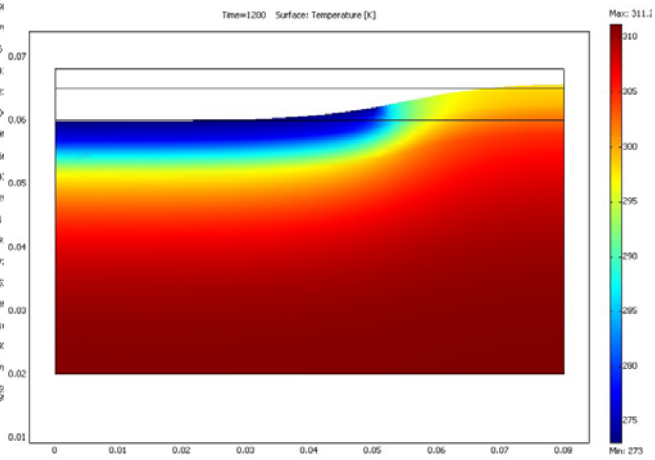

Figure 6: Temperature profile after 20 minutes of cooling.

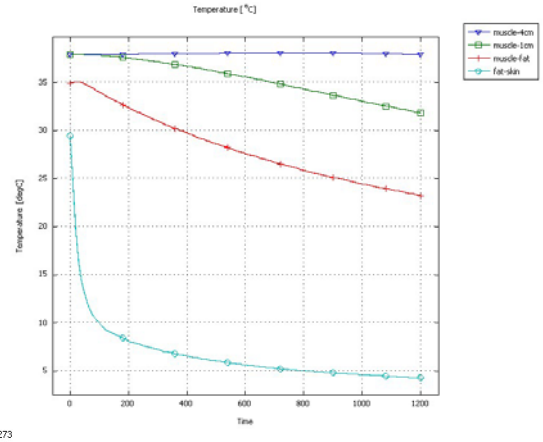

Figure 7: The temperature (^{o}C) vs. time (seconds) at different layers after 1200s of cooling.

Cycles:

After the 20 minute cooling process was completed, we studied the effect of the subsequent 20 minute warming cycle (at room temperature). The skin and muscle absorbed heat from the surrounding and the temperature profile changed. Following the absorption of heat, the muscle layer expanded and the swelling returned (**Figures 8 & 9**). From the temperature vs. time data (**Figure 10**), we were able to observe the increase in temperature at the skin-fat and fat-muscle layers. However, at 1 cm and 4 cm into the muscle layer, the temperature drop continued during the warming cycle.

Following the warming cycle, another 1200 seconds cooling cycle took place. Figures 10 – 13 show the temperature changes during this cycle.

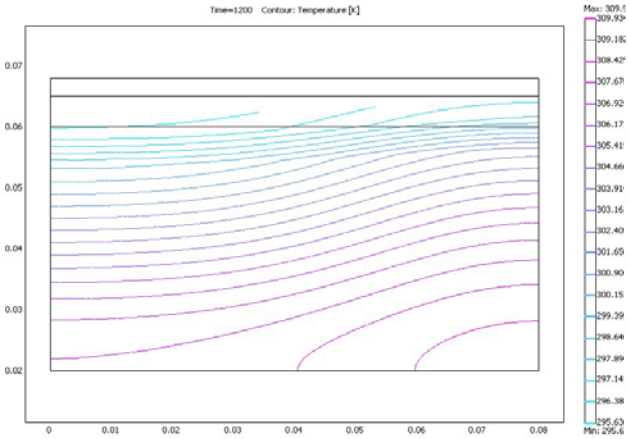

Figure 8: Temperature contour at time = 2400 seconds. 1200 seconds of warming in room temperature after initial cooling step.

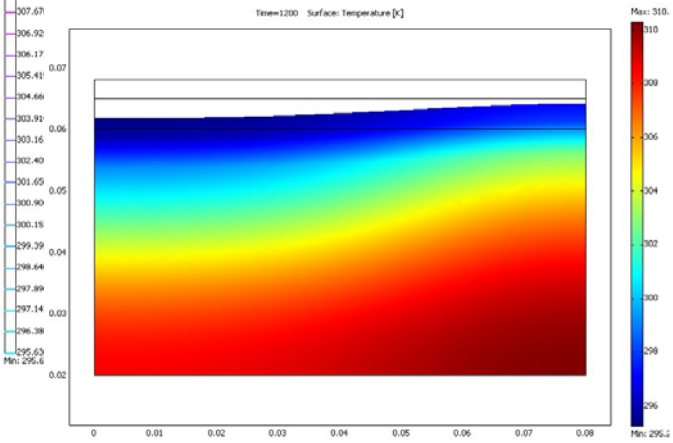

Figure 9: Temperature profile at time = 2400 seconds. 1200 seconds of warming in room temperature after initial cooling step.

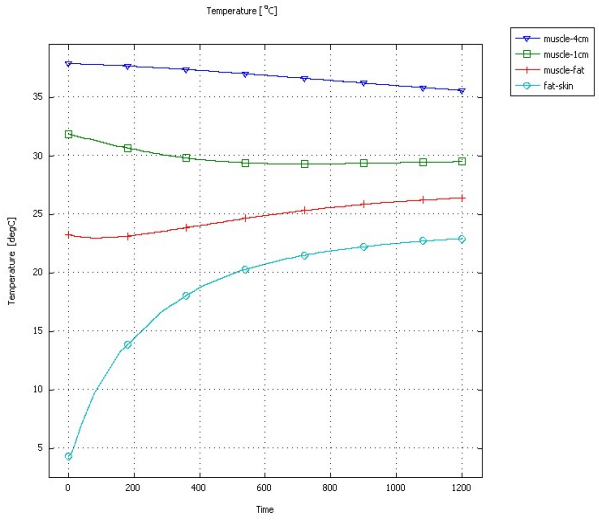

Figure 10: The temperature (^{o}C) vs. time (seconds) at different layers after 1200s of cooling.

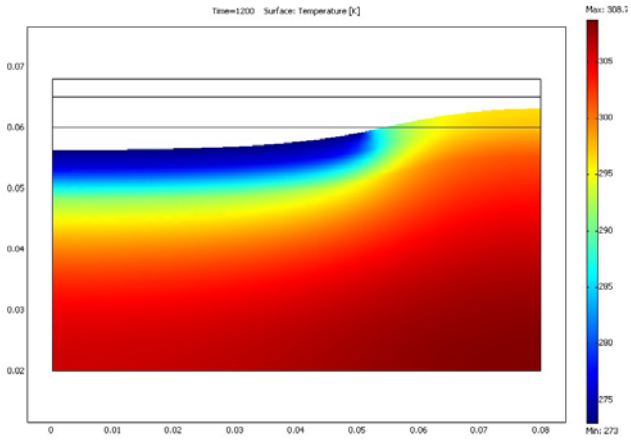

Figure 12: Temperature profile at time = 3600 seconds. 1200 seconds of cooling after initial warming step.

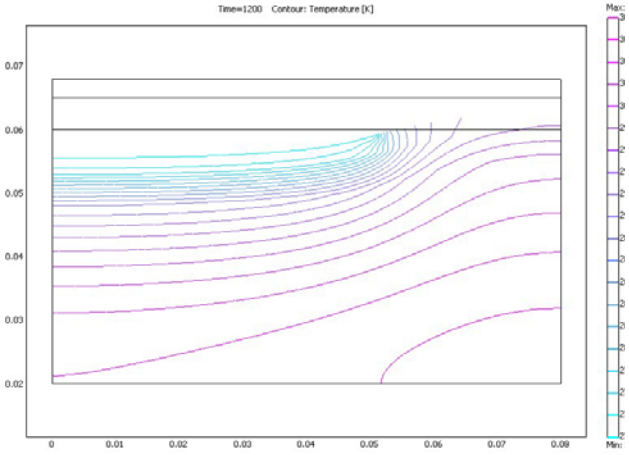

Figure 11: Temperature contour at time = 3600 seconds. 1200 seconds of cooling after initial warming step.

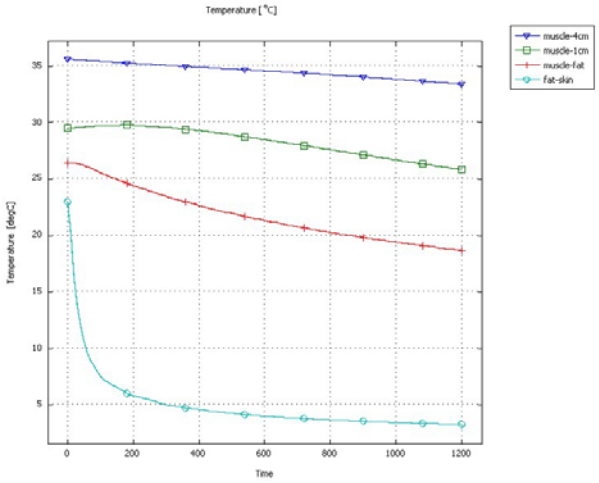

Figure 13: The temperature (^{o}C) vs. time (seconds) at different layers after another 1200s of cooling, which followed the 1200 of warming.

Sensitivity Analysis

Varying Material Properties

In the sensitivity analysis, we determined the responsiveness of the model to +/- 10% variations in several key parameters, such as specific heat, density, thermal conductivity and mesh. By using COMSOL, we modeled the temperature profile and the temperature of a node 1 cm below the fat-muscle boundary throughout the heating and cooling cycle. The results of our sensitivity analysis with varying parameters were recorded in the table below:

	Temp (1cm deep) K	
	1200 (s)	2400 (s)
K +10%	304.2549	302.2333
K -10%	305.6511	303.0747
ρ +10%	305.6074	302.8844
ρ -10%	304.2412	302.2568
Cp +10%	305.6494	302.8423
Cp -10%	304.5251	302.4101
Refined Mesh	305.1421	302.7246

Table 2: Results of sensitivity analysis. K, ρ and Cp were varied by +/- 10% of the values used to compute complete solutions. The temperature at 1 cm below the fat-muscle layer was recorded.

Based on the temperature data recorded from the sensitivity analysis, we observed no significant changes. The variations of +/- 10% of the material properties did not contribute to significant changes in temperature profile. For the refined mesh, no observable difference was recorded as well.

In **Figures 14-16**, the temperature profiles for Cp – 10% at the end of three cycles were recorded. The trend of the temperature profile is the same as the trend observed in our complete solution. The variation of other material properties showed the same trend (see **Appendix** for individual temperature profiles: Figures A1-A15).

The sensitivity analysis showed that the desirable cooling of 10 to 15^{o}C was achieved at the end of the complete 3600 seconds cycle in 1 cm below the fat-muscle layer, and that varying the parameters by 10% do not affect the effectiveness of this treatment.

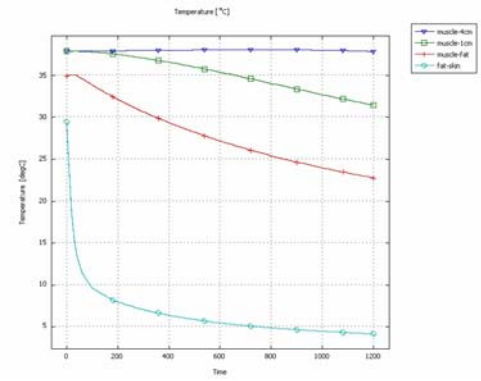

Figure 14: The temperature profile at different locations throughout the first cooling cycle for Cp – 10% (0s to 1200s)

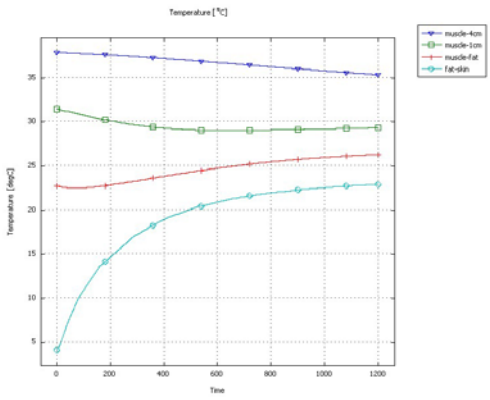

Figure 15: The temperature profile at different locations throughout the warming cycle for Cp – 10% (1200s to 2400s)

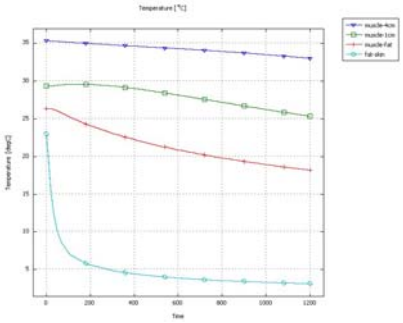

Figure 16: The temperature profile at different locations throughout the second cooling cycle for Cp –10%(2400s to 3600s

Contracting Muscle Layer vs. Non-Contracting Muscle Layer

When moving mesh condition is employed, the COMSOL solver automatically re-mesh the model geometry every time step. Therefore it is not practical to measure a temperature change of a certain point by tracking the nearest node.

Instead, we used contour plot to find out the temperature. We located the closest isotherm for a point 3cm above from the bottom of the muscle layer (consequently 1cm below the muscle-fat boundary). The results are following:

Time	600 (sec)	900 (sec)	1200 (sec)
Non-Moving Mesh	306.203 K	303.957 K	302.43 K
Moving Mesh	306.203 K	302.428 K	297.844 K

Table 3: Temperature at 3cm above from the bottom of the muscle layer for moving mesh model and non-moving mesh model at different time points.

10 Minutes Cycle

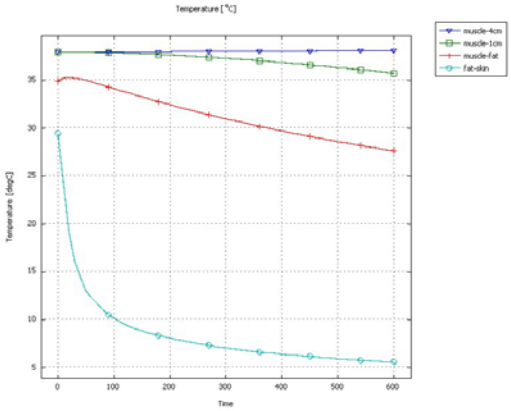

Figure 17: Temperature Change from 0 to 600 seconds (cooling)

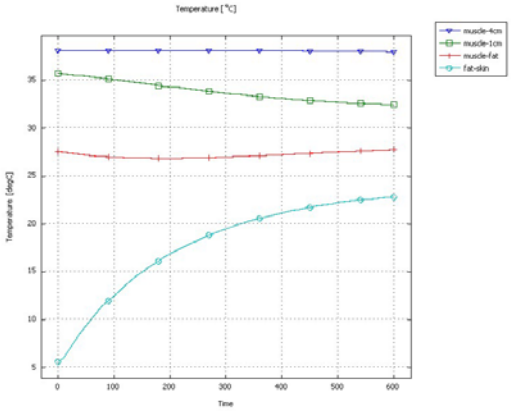

Figure 18: Temperature Change from 600 to 1200 seconds (warming)

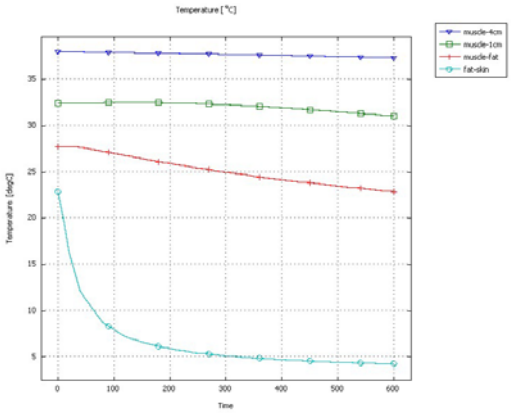

Figure 19: Temperature Change from 1200 to 2400 seconds (cooling)

The temperature change in a contracting muscle for a 10 minute cooling and warming cycle is not as pronounced as in the 20 minutes cycle (**Figure 17 – 19**). The overall temperature drop after the cycle was 6 ^{o}C, which was not close to the desirable 10 to 15 ^{o}C drop.

Fat Layer Muscle

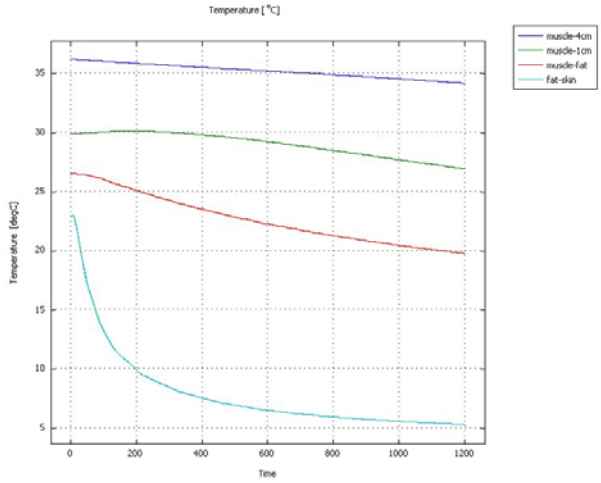

Figure 20: Temperature Change from 2400 to 3600 seconds (cooling) with +50% fat layer thickness.

In the final sensitivity analysis test, we increased the fat layer thickness of the model by 50% (from 5mm to 7.5mm). It was seen that the temperature change in the final 20 minutes of the cycle (**Figure 20**) was the same as in the previous studies. The final temperature at 1 cm below fat-muscle layer turned out to be about 27^{o}C.

Mesh Convergence

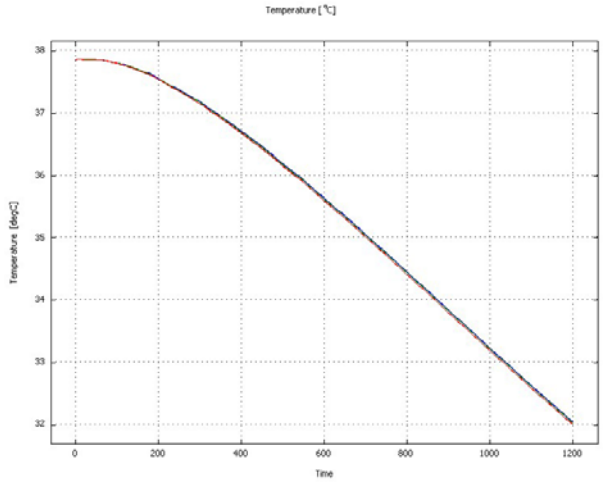

Figure 21: Temperature profile at the end of first cooling stage of models with 617 Nodes, 2468 nodes and 9872 nodes.

Based on our mesh convergence analysis (**Figure 21**), we observed no difference in the modeling of temperature profile at 617 nodes, 2468 nodes and 9872 nodes. Hence, it was concluded that the original mesh was sufficient for our model.

Conclusion and Design Recommendation:

Interpretation of Results

Based on the results obtained in this study, we found that the desirable temperature drop of 10^{o}C was achieved only at the proximity of the fat-muscle layer at the end of a 20 minutes cooling cycle. In order to achieve the desirable cooling at the distance of 1 cm below the fat-muscle layer, a cycle of 20 minutes cooling, 20 minutes warming and 20 minutes cooling must be carried out. The overall temperature decrease over this hour long cycle was about 11^{o}C at 1 cm below the fat-muscle layer.

In the sensitivity analysis, K, ρ and Cp were varied by +/- 10%, and the temperature variations at 1 cm below the fat-muscle layer were recorded. The difference between the + 10% and -10% was by less than one percent, so we can safely conclude that the variation of material properties will not affect the change of temperature by a significant amount. Also, by looking at the temperature 1 cm below fat-muscle layer after 3600s, we can also see that the desirable temperature drop of 10^{o}C was reached for each of the variations.

In the comparison of the contracting vs. non-contracting muscle layer, we observed that the overall temperature drop of a contracting muscle layer had a greater temperature change and reached a lower temperature by the end of the cooling and warming cycle. Based on the results presented by Table 3, it is clear to see that the contracting model cools the muscle more in the cooling process.

To compare the desirable cooling and warming cycle, we compared the results from 20 minutes cycle to the results from 10 minutes cycle. We found that the final temperature at 1 cm below fat-muscle layer by the end of 10 minutes cooling, 10 minutes warming and 10 minutes cooling did not reach the desired temperature. Thus, we conclude that the 20 minutes cycle model is better for treating injury.

Finally, in the study in which we increased the fat layer by 50%, we observed no change in the trend of temperature changes. However, the final temperature at the muscle 1 cm below the fat-muscle layer turned out to be 1 ^{o}C higher than the final temperature at the same location with the original fat layer. This was expected, due to the additional insulating properties of a thicker fat layer. Even though the temperature turned out to be higher for a thicker fat layer, the desirable lowering of temperature by 10^{o}C was still achieved.

Problems Encountered

The modeling of constriction of muscle upon ice cooling required implementation of a moving boundary and mesh. Unfortunately, we could not successfully incorporate the thermal constriction into FIDAP, because FIDAP cannot model an elastic solid, though this problem could have been addressed by defining the muscle layer as fluid with very high viscosity. However, we chose not to pursue that option and decided to model using another finite element software package, COMSOL Multiphysics. With the more user-friendly interface and capability to model a moving mesh, we could come up with a reliable solution for simulating the cooling of injured muscle.

Defining the mathematics of thermal constriction was another challenge. The literature on this subject is rather limited; sports medicine journals were our primary sources in our literature search. However, studies in the field were generally heuristic, lacking mathematical explanations on the process. While there were some studies on effect of temperature change on vascular dilation in muscle which were more mathematically oriented, the relationship between a single blood vessel and a whole muscle was not discussed.

Design Recommendations

Our model found that after 60 minutes of a "20 minute on, 20 minute off" cycle, the desired temperature drop of 10°C was achieved 1 cm deep into the muscle layer. While this method does achieve the desired cooling, there is still room for improvement. We therefore recommend looking into other forms of cooling or different timing cycles. For example, using cold running water over the leg may provide a quicker cooling of the deep muscle tissues than using an ice pack. Similarly if the ice is applied for longer it may be possible to cool deeper into the muscle. However, the therapy as presented in this report, is a convenient and cheap method of cooling some of the muscle.

Realistic Constraints

Our model of the cooling of a swelled, injured muscle has some important constraints in design which must be considered. The most important constraint stems from the many differences individuals possess- different individuals have muscles of vastly differing sizes. Additionally, individuals have different rates of metabolism, and hence heat generation and blood flow rates, all based on a myriad of factors such as age, lifestyle, and genetic factors. Hence, we must consider the impossibility of modeling these physical factors over a general population to be important constraint in our design.

Another important constraint of our design, safety, follows from the impossibility of modeling a cooling technique for all populations. Safety is an important factor that must be considered in the application of our model; while our modeled method of treatment may work perfectly for a robust adult, it may be too extreme for a child, cooling muscles beyond healthy temperatures. Hence, though our model is good for explaining a general observed phenomenon of the cooling/heating cycles, the direct application of the technique should be carefully monitored for each individual in order to ensure the safe treatment of an injured muscle.

As this therapy only involves freezing water and putting it in a plastic bag, there are no significant manufacturing, economic, social, ethical or environmental problems with it. One can recycle the plastic bag and the melted ice is of no problem to the environment. As mentioned above, the only concern about this therapy is personal safety. However this can be easily dealt with by simply removing the ice if discomfort from it is too great.

APPENDIX A

Governing Equations:

$$\rho c_p \left(\frac{\partial T}{\partial t} = k\left(\frac{1}{r}\frac{\partial}{\partial r}\left(r\frac{\partial T}{\partial r}\right) + \frac{\partial^2 T}{\partial z^2}\right) + Q\right.$$

The governing equation that our project is based on is shown above. There is no convection of heat transfer involved in this project; thus, the convection turn in the equation is effectively entered as zero during the programming process.

Initial Conditions:

$T_{ice} = 273$ K
T_{skin} (t = 0, 0 < z < 0.3 cm) = 305 K
T_{fat} (t = 0, 0.3 cm < z < 0.8 cm) = 307 K
T_{muscle} (t = 0, 0.8 cm < z < 6.8 cm) = 310 K
$T_{blood} = 310$ K

Assumption: All tissues are at body temperature (310 K).

Moving Mesh Conditions:

Bottom: Mesh displacement = 0
Muscle Sides: Radial mesh velocity = 0
Skin, fat side, skin top, fat-skin-free boundary
At t = 0, the muscle is in swelled state. The thickness of the muscle is a function of the temperature given as follows:

$$dL = L_0 * \alpha * dT$$

Muscle-fat = normal velocity = 0.007*(dT/dt)

In previous cryotherapy for sporting injury studies, an approximated 0.5 to 1cm of decrease in swelling was observed for sporting trauma after 20 minutes of cold therapy. Due to the lack of research on the formulation of a mathematical model that simulates the decrease in swelling with respect to temperature different temperature, we assumed that after 20 minutes of our cold therapy, the decrease in swelling will be around that range. By trial and error, we determined that the previous mentioned input will yield a reasonable model for this process. We modeled our project and the moving boundary based on these knowledge and assumptions.

Boundary Conditions:

$T\big\|_{z=0} = 273K$	Temperature of ice is a boundary condition for the skin surface for t = 0-20 minutes and for t = 40-60 minutes.
$T\big\|_{z=0} = 296K$	Temperature of skin surface for t = 20-40 minutes (warming cycle). Upon the removal of ice, the skin is exposed to room temperature at 296K.
$\left.\frac{\partial T}{\partial z}\right\|_{0.05<r<0.08} = 0$	Heat flux on the skin layer that's not cover by the ice pack
$\left.\frac{\partial T}{\partial z}\right\|_{z=L} = 0$	Heat flux on the bottom boundary of muscle is zero assuming bone an insulator. L is the estimated depth of our ice-plastic-tissue model, which is 6.8 cm.
$\left.\frac{\partial T}{\partial r}\right\|_{r=0} = 0$	Heat flux along the axis of symmetry is zero.
$\left.\frac{\partial T}{\partial z}\right\|_{r=0.08} = 0$	Heat flux on the outside boundary of our cylinder is zero

Input Parameters:

Length of radius: 5 cm
Thickness of skin (sum of epidermis, dermis, subcutaneous tissue): 3 mm
Thickness of fat: 5 mm
Thickness of muscle (hamstring): 6 cm

At t = 0, the muscle is in swelled state. The thickness of the muscle is a function of the temperature (and hence, time), and shrinks as the temperature decreases.

Thermal Properties:

Table A-1. Thermal properties of ice, plastic, and tissues modeled in the experiment.

Material Type	Initial Temp (K)	k (W/m·K)	c_p (kJ/kg·K)	ρ (kg/m^3)
Ice	273	-	-	-
Skin	310	0.29	3.39	1030
Fat	310	0.204	2.43	938
Muscle	310	0.42	3.55	1044

Metabolic Heat Generation in human leg = 1.1 kW/m^3

Assumption: All thermal properties of our materials and tissues are constant

APPENDIX B

COMSOL Code:

```
% COMSOL Multiphysics
Model M-file
% Generated by COMSOL
3.2 (COMSOL 3.2.0.222,
$Date: 2005/09/01
18:02:30 $)
% Some geometry objects
are stored in a separate
file.
% The name of this file
is given by the variable
'flbinaryfile'.

flclear fem

% COMSOL version
clear vrsn
vrsn.name = 'COMSOL 3.2';
vrsn.ext = '';
vrsn.major = 0;
vrsn.build = 222;
vrsn.rcs = '$Name:  $';
vrsn.date = '$Date:
2005/09/01 18:02:30 $';
fem.version = vrsn;

flbinaryfile='skinmoving
.mphm';

% Geometry
clear draw
g10=flbinary('g10','draw
',flbinaryfile);
g9=flbinary('g9','draw',
flbinaryfile);
g12=flbinary('g12','draw
',flbinaryfile);
g8=flbinary('g8','draw',
flbinaryfile);
g11=flbinary('g11','draw
',flbinaryfile);
draw.p.objs =
{g10,g9,g12,g8,g11};
draw.p.name =
{'PT3','PT2','PT5','PT1'
,'PT4'};
draw.p.tags =
{'g10','g9','g12','g8','
g11'};
g6=flbinary('g6','draw',
flbinaryfile);
g2=flbinary('g2','draw',
flbinaryfile);
g7=flbinary('g7','draw',
flbinaryfile);
draw.s.objs = {g6,g2,g7};
draw.s.name =
{'R2','R1','R3'};
draw.s.tags =
{'g6','g2','g7'};
fem.draw = draw;
fem.geom = geomcsg(fem);

% Initialize mesh
fem.mesh=meshinit(fem);

% (Default values are
not included)


% Application mode 1
clear appl
appl.mode.class =
'MovingMesh';
appl.mode.type = 'axi';
appl.dim = {'dr','dz'};
appl.sdim =
{'R','PHI','Z'};
appl.shape =
{'shlag(2,''lm1'')','shl
ag(2,''lm2'')','shlag(2,
''r'')','shlag(2,''z'')'
};
appl.gporder = 4;
appl.cporder = 2;
appl.border = 'on';
appl.assignsuffix =
'_ale';
clear prop
prop.analysis='transient
';
appl.prop = prop;
clear bnd
bnd.defflag =
{{0;0},{1;1},{0;0},{0;0}
};
bnd.type =
{'vel','def','vel','def'
};
bnd.veldefflag =
{{1;0},{0;0},{1;0},{0;0}
};
bnd.constrcoord =
{'global','global','loca
l','global'};
bnd.wcshape = [1;2];
bnd.veldeform =
{{0;0},{0;0},{'0.0007*TT
IME';'T*3e-8-18e-
6'},{0;0}};
bnd.ind =
[1,2,1,3,1,4,4,2,3,4,4,1
,1,1];
appl.bnd = bnd;
clear equ
equ.shape = [3;4];
equ.ind = [1,1,1];
appl.equ = equ;
fem.appl{1} = appl;

% Application mode 2
clear appl
appl.mode.class =
'HeatTransfer';
appl.mode.type = 'axi';
appl.border = 'on';
appl.assignsuffix =
'_ht';
clear prop
clear weakconstr
weakconstr.value = 'off';
weakconstr.dim = {'lm5'};
prop.weakconstr =
weakconstr;
appl.prop = prop;
clear bnd
bnd.type =
{'ax','q0','cont','cont'
,'q','T'};
bnd.h = {0,0,0,0,50,50};
bnd.T0 =
{0,0,273,0,273,273};
bnd.Tinf =
{0,0,0,0,293,293};
bnd.ind =
[1,2,1,3,1,4,6,2,3,4,5,2
,2,2];
appl.bnd = bnd;
clear equ
equ.k = {0.43,0.2,0.63};
equ.init = {311,305,300};
equ.rho =
{1044,938,1030};
equ.C = {3550,2430,3790};
equ.Q = 1100;
equ.ind = [1,2,3];
appl.equ = equ;
fem.appl{2} = appl;
fem.sdim =
{{'R','Z'},{'r','z'}};
fem.frame = {'rz','ale'};
fem.border = 1;
fem.units = 'SI';

% Multiphysics
fem=multiphysics(fem);

% Extend mesh
fem.xmesh=meshextend(fem
);

% Solve problem
fem.sol=femtime(fem, ...

'solcomp',{'z','r','T','
lm2','lm1'}, ...

'outcomp',{'z','r','T','
lm2','lm1'}, ...

'tlist',[0:10:1200], ...

'tout','tlist');

% Save current fem
structure for restart
purposes
fem0=fem;

% Plot solution
postplot(fem, ...
```

```
'tridata',{'T','cont','i
nternal'}, ...

'trimap','jet(1024)',  ...

'solnum','end', ...

'title','Time=1200
Surface: Temperature
[K]', ...
         'refine',3, ...
         'axis',[-
0.00399999991059303,0.08
39999981224537,0.0116666
690135995,0.076333334234
8536,-1,1]);

% Plot in cross-section
or along domain
postcrossplot(fem,0,[5,6
,7,8], ...

'pointdata','T', ...

'title','Temperature
[<sup>o</sup>C]', ...

'axislabel',{'Time','Tem
perature  [degC]'}, ...

'refine',3);

% (Default values are
not included)

% Application mode 1
clear appl
appl.mode.class =
'MovingMesh';
appl.mode.type = 'axi';
appl.dim = {'dr','dz'};
appl.sdim =
{'R','PHI','Z'};
appl.shape =
{'shlag(2,''lm1'')','shl
ag(2,''lm2'')','shlag(2,
''r'')','shlag(2,''z'')'
};
appl.gporder = 4;
appl.cporder = 2;
appl.border = 'on';
appl.assignsuffix =
'_ale';
clear prop
prop.analysis='transient
';
appl.prop = prop;
clear bnd
bnd.defflag =
{{0;0},{1;1},{0;0},{0;0}
};
bnd.type =
{'vel','def','vel','def'
};
bnd.veldefflag =
{{1;0},{0;0},{1;0},{0;0}
};
bnd.constrcoord =
{'global','global','loca
l','global'};
bnd.wcshape = [1;2];
bnd.veldeform =
{{0;0},{0;0},{'0.0007*TT
IME';'T*3e-8-18e-
6'},{0;0}};
bnd.ind =
[1,2,1,3,1,4,4,2,3,4,4,1
,1,1];
appl.bnd = bnd;
clear equ
equ.shape = [3;4];
equ.ind = [1,1,1];
appl.equ = equ;
fem.appl{1} = appl;

% Application mode 2
clear appl
appl.mode.class =
'HeatTransfer';
appl.mode.type = 'axi';
appl.border = 'on';
appl.assignsuffix =
'_ht';
clear prop
clear weakconstr
weakconstr.value = 'off';
weakconstr.dim = {'lm5'};
prop.weakconstr =
weakconstr;
appl.prop = prop;
clear bnd
bnd.type =
{'ax','q0','cont','cont'
,'q'};
bnd.h = {0,0,0,0,50};
bnd.T0 = {0,0,273,0,273};
bnd.Tinf = {0,0,0,0,293};
bnd.ind =
[1,2,1,3,1,4,5,2,3,4,5,2
,2,2];
appl.bnd = bnd;
clear equ
equ.k = {0.43,0.2,0.63};
equ.init = {311,305,300};
equ.rho =
{1044,938,1030};
equ.C = {3550,2430,3790};
equ.Q = 1100;
equ.ind = [1,2,3];
appl.equ = equ;
fem.appl{2} = appl;
fem.sdim =
{{'R','Z'},{'r','z'}};
fem.frame = {'rz','ale'};
fem.border = 1;
fem.units = 'SI';

% Multiphysics
fem=multiphysics(fem);

% Extend mesh
fem.xmesh=meshextend(fem
);

% Solve problem
fem.sol=femtime(fem, ...

'init',fem0.sol, ...

'solcomp',{'z','r','T','
lm2','lm1'}, ...

'outcomp',{'z','r','T','
lm2','lm1'}, ...

'tlist',[0:10:1200], ...

'tout','tlist');

% Save current fem
structure for restart
purposes
fem0=fem;

% Plot solution
postplot(fem, ...

'tridata',{'T','cont','i
nternal'}, ...

'trimap','jet(1024)',  ...

'solnum','end', ...

'title','Time=1200
Surface: Temperature
[K]', ...
         'refine',3, ...
         'axis',[-
0.00612935593440642,0.08
61293541462671,0.0120299
648856291,0.075970038362
8241,-1,1]);

% Plot in cross-section
or along domain
postcrossplot(fem,0,[5,6
,7,8], ...

'pointdata','T', ...

'title','Temperature
[<sup>o</sup>C]', ...

'axislabel',{'Time','Tem
perature  [degC]'}, ...

'refine',3);

% (Default values are
not included)

% Application mode 1
clear appl
appl.mode.class =
'MovingMesh';
appl.mode.type = 'axi';
appl.dim = {'dr','dz'};
appl.sdim =
{'R','PHI','Z'};
appl.shape =
{'shlag(2,''lm1'')','shl
ag(2,''lm2'')','shlag(2,
''r'')','shlag(2,''z'')'
};
appl.gporder = 4;
appl.cporder = 2;
appl.border = 'on';
appl.assignsuffix =
'_ale';
clear prop
```

```
prop.analysis='transient
';
appl.prop = prop;
clear bnd
bnd.defflag =
{{0;0},{1;1},{0;0},{0;0}
};
bnd.type =
{'vel','def','vel','def'
};
bnd.veldefflag =
{{1;0},{0;0},{1;0},{0;0}
};
bnd.constrcoord =
{'global','global','loca
l','global'};
bnd.wcshape = [1;2];
bnd.veldeform =
{{0;0},{0;0},{'0.0007*TT
IME';'T*3e-8-18e-
6'},{0;0}};
bnd.ind =
[1,2,1,3,1,4,4,2,3,4,4,1
,1,1];
appl.bnd = bnd;
clear equ
equ.shape = [3;4];
equ.ind = [1,1,1];
appl.equ = equ;
fem.appl{1} = appl;

% Application mode 2
clear appl
appl.mode.class =
'HeatTransfer';
appl.mode.type = 'axi';
appl.border = 'on';
appl.assignsuffix =
'_ht';
clear prop
clear weakconstr
weakconstr.value = 'off';
weakconstr.dim = {'lm5'};
prop.weakconstr =
weakconstr;
appl.prop = prop;
clear bnd
bnd.type =
{'ax','q0','cont','cont'
,'q','T'};
bnd.h = {0,0,0,0,50,50};
bnd.T0 =
{0,0,273,0,273,273};
bnd.Tinf =
{0,0,0,0,293,293};
bnd.ind =
[1,2,1,3,1,4,6,2,3,4,5,2
,2,2];
appl.bnd = bnd;
clear equ
equ.k = {0.43,0.2,0.63};
equ.init = {311,305,300};
equ.rho =
{1044,938,1030};
equ.C = {3550,2430,3790};
equ.Q = 1100;
equ.ind = [1,2,3];
appl.equ = equ;
fem.appl{2} = appl;
fem.sdim =
{{'R','Z'},{'r','z'}};
fem.frame = {'rz','ale'};
fem.border = 1;
fem.units = 'SI';

% Multiphysics
fem=multiphysics(fem);

% Extend mesh
fem.xmesh=meshextend(fem
);
% Solve problem
fem.sol=femtime(fem, ...

'init',fem0.sol, ...

'solcomp',{'z','r','T','
lm2','lm1'}, ...

'outcomp',{'z','r','T','
lm2','lm1'}, ...

'tlist',[0:10:1200], ...

'tout','tlist');

% Save current fem
structure for restart
purposes
fem0=fem;

% Plot solution
postplot(fem, ...

'tridata',{'T','cont','i
nternal'}, ...

'trimap','jet(1024)',  ...

'solnum','end', ...

'title','Time=1200
Surface: Temperature
[K]', ...
         'refine',3, ...
         'axis',[-
0.00612935593440642,0.08
61293541462671,0.0120299
648856291,0.075970038362
8241,-1,1]);
```

APPENDIX C

Please find additional graphs for Sensitivity Analysis below:

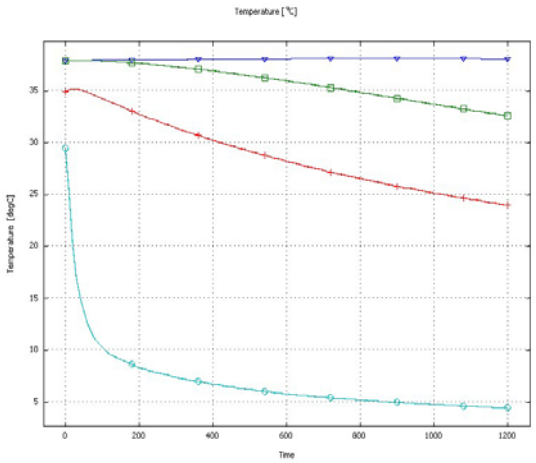

Figure C-1: The temperature profile at different locations throughout the first cooling cycle for K – 10%(0s to 1200s)

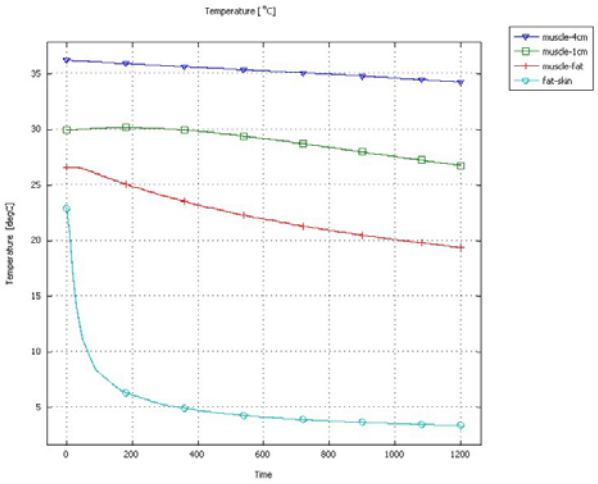

Figure C-3: The temperature profile at different locations throughout the second cooling cycle for K – 10%(2400s to 3600s)

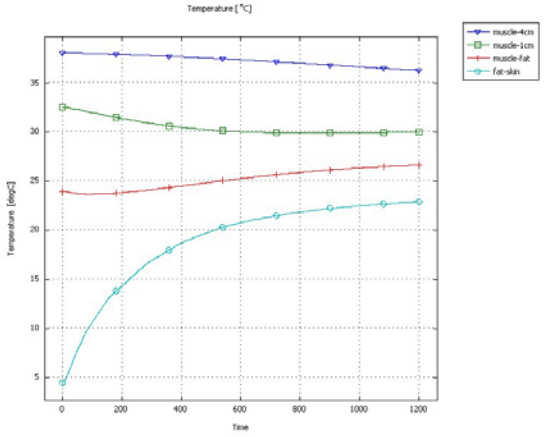

Figure C-2: The temperature profile at different locations throughout the warming cycle for K – 10%(1200s to 2400s)

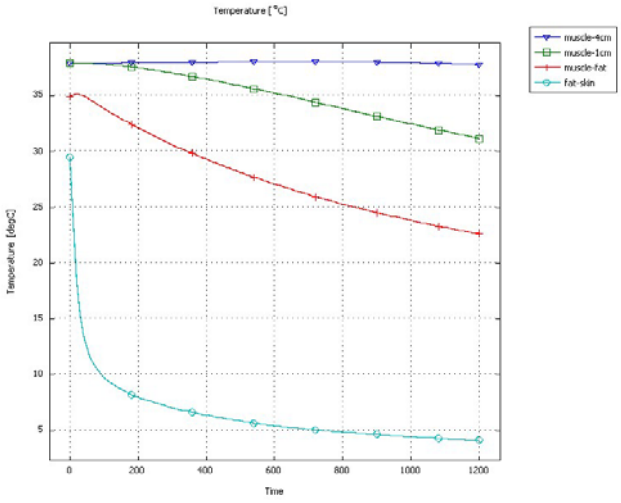

Figure C-4: The temperature profile at different locations throughout the first cooling cycle for K +10%(0s to 1200s)

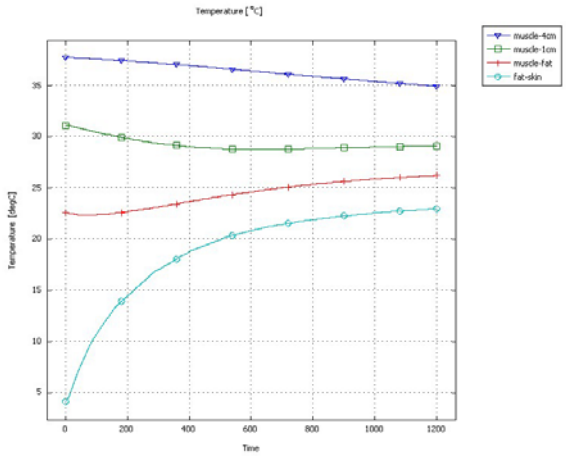

Figure C-5: The temperature profile at different locations throughout the warming cycle for K +10%(1200s to 2400s)

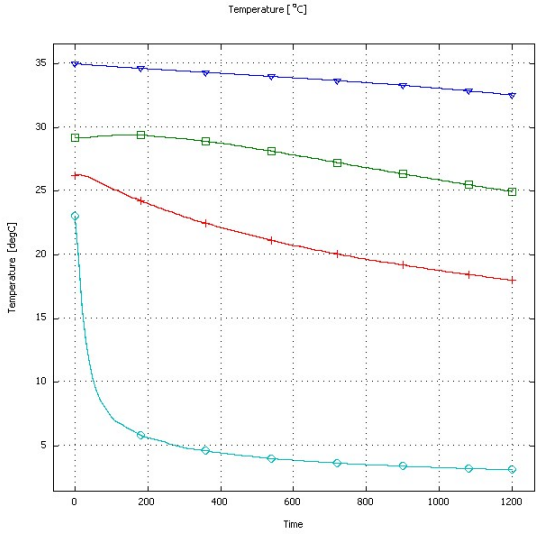

Figure C-6: The temperature profile at different locations throughout the second cooling cycle for K +10%(2400s to 3600s)

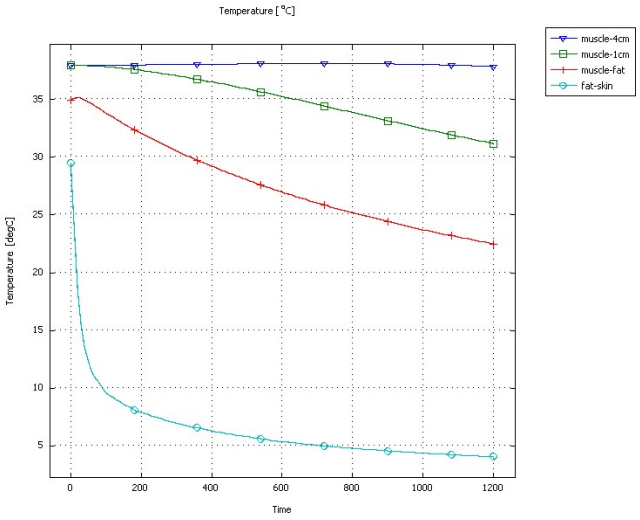

Figure C-7: The temperature profile at different locations throughout the first cooling cycle for ρ - 10%(0s to 1200s)

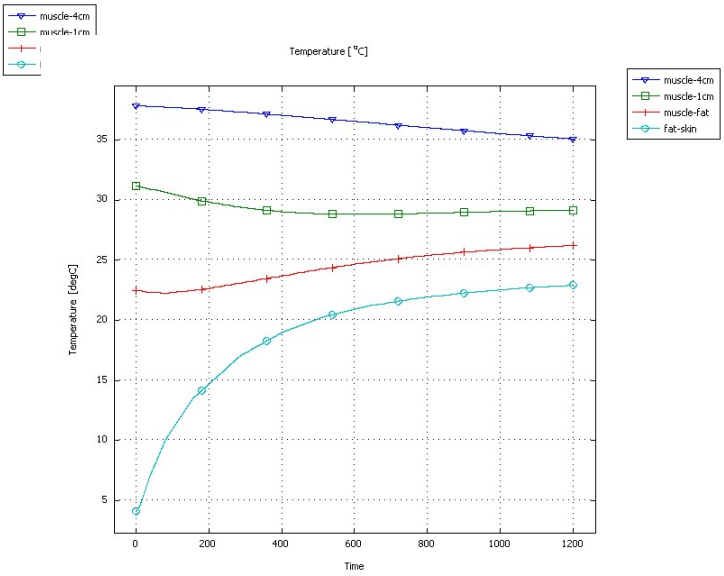

Figure C-8: The temperature profile at different locations throughout the warming cycle for ρ -10%(1200s to 2400s)

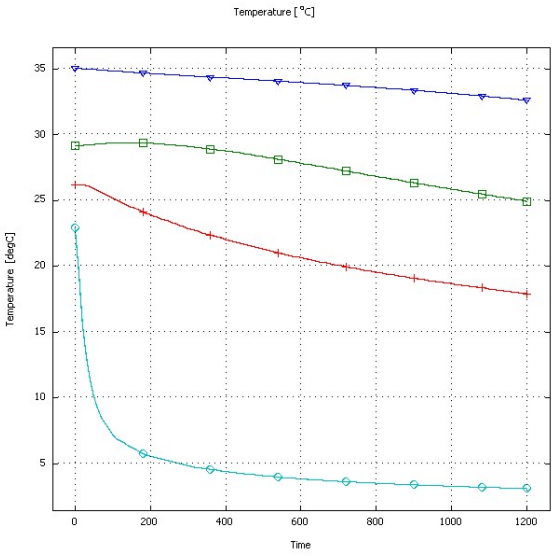

Figure C-9: The temperature profile at different locations throughout the second cooling cycle for ρ - 10%(2400s to 3600s)

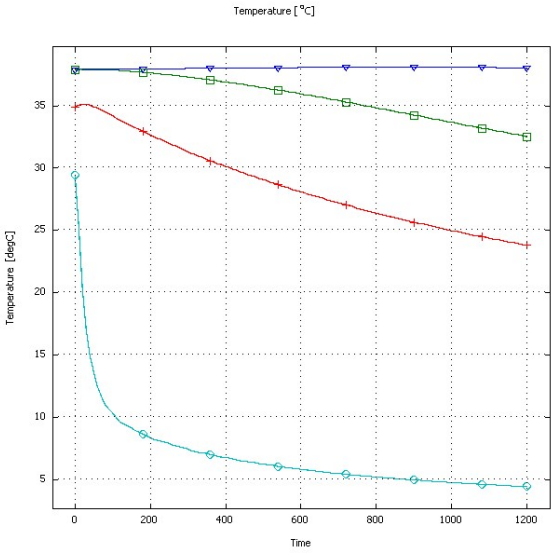

Figure C-10: The temperature profile at different locations throughout the first cooling cycle for ρ +10%(0s to 1200s)

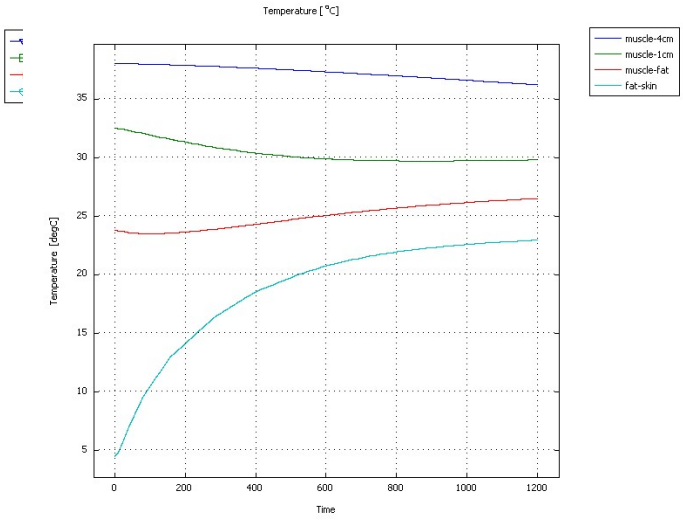

Figure C-11: The temperature profile at different locations throughout the warming cycle for ρ +10%(1200s to 2400s)

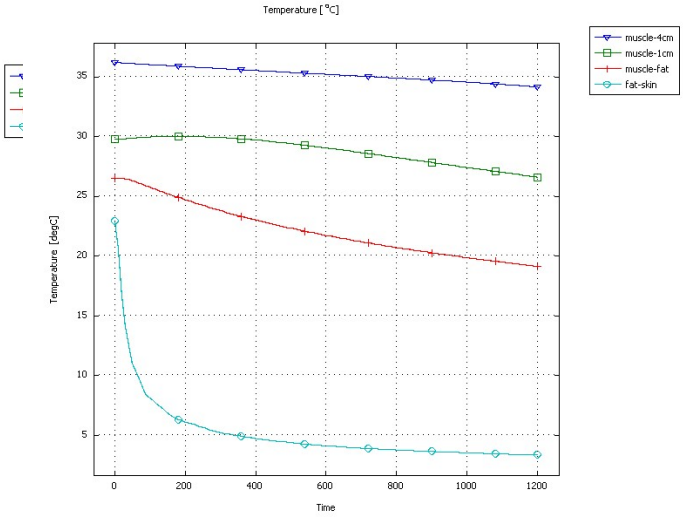

Figure C-12: The temperature profile at different locations throughout the first cooling cycle for ρ +10%(2400s to 3600s)

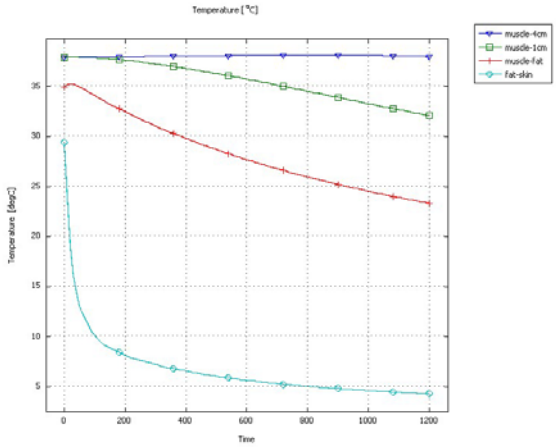

Figure C-13: The temperature profile at different locations throughout the first cooling cycle for refined mesh (0s to 1200s)

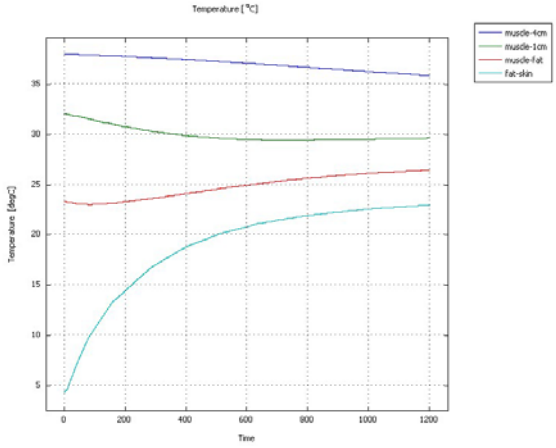

Figure C-14: The temperature profile at different locations throughout the warming cycle for refined mesh (1200s to 2400s)

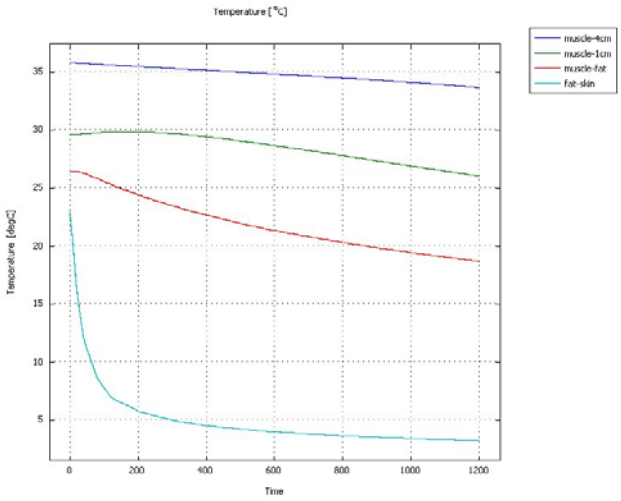

Figure C-15: The temperature profile at different locations throughout the second cooling cycle for refined mesh (2400s to 3600s)

APPENDIX D

References:

Gowrishankar, TR, Stewart, DA, Martin, GT, Weaver, JC. "Transport lattice models of heat transport in skin with spatially heterogeneous, temperature dependent perfusion." *BioMedical Engineering OnLine*. 2004 March; 3:42.

Elert, G. "The Physics Hpertextbook." <http://hypertextbook.com/physics/>. Updated 2006. Accessed February 19, 2006.

Giering K, Minet O, Lamprecht I and Muller G. "Review of thermal properties of biological tissues." *Laser Induced Interstitial Thermotherapy*. 1995; p 45-65.

ACKNOWLEGEMENT

We would like to thank Professor Datta and Vineet Rakesh for their constant encouragement and help throughout the semester. The valuable advices we received during this semester were critical for the development of this project and education. Also, we would like to thank Amit Halder for allowing us to access COMSOL with his computer.